Article

Crystal-Like Atomic Arrangement and Optical Properties of 25La$_2$O$_3$−75MoO$_3$ Binary Glasses Composed of Isolated MoO$_4^{2-}$

Atsunobu Masuno,* Sae Munakata, Yoshihiro Okamoto, Toyonari Yaji, Yoshihisa Kosugi, and Yuichi Shimakawa

Read Online

ACCESS | Metrics & More | Article Recommendations

ABSTRACT: Transparent and brown La$_2$O$_3$−MoO$_3$ binary glasses were prepared in bulk form using a levitation technique. The glass-forming range was limited, with the primary composition being approximately 25 mol % La$_2$O$_3$. The 25La$_2$O$_3$−75MoO$_3$ glass exhibited a clear crystallization at 546 °C, while determining its glass transition temperature was difficult. Notably, despite its amorphous nature, the glass possessed a density and packing density comparable to those of crystalline La$_2$Mo$_3$O$_{12}$. X-ray absorption fine structure and Raman scattering analyses revealed that the glass structure closely resembles La$_2$Mo$_3$O$_{12}$ due to the presence of isolated MoO$_4^{2-}$ units, whereas disordered atomic arrangement around La atoms was confirmed. The glass demonstrated transparency ranging from 378 to 5500 nm, and

the refractive index at 1.0 μm was estimated to be 2.0. The optical bandgap energy was 3.46 eV, which was slightly smaller than that of La$_2$Mo$_3$O$_{12}$. Additionally, the glass displayed a transparent region ranging from 6.5 to 8.0 μm. This occurrence results from the decreased diversity of MoO$_n$ units and connectivity of Mo−O−Mo, which resulted in the reduced overlap of multiphonon absorption. This glass formation, with its departure from conventional glass-forming rules, resulted in distinctive glasses with crystal-like atomic arrangements.
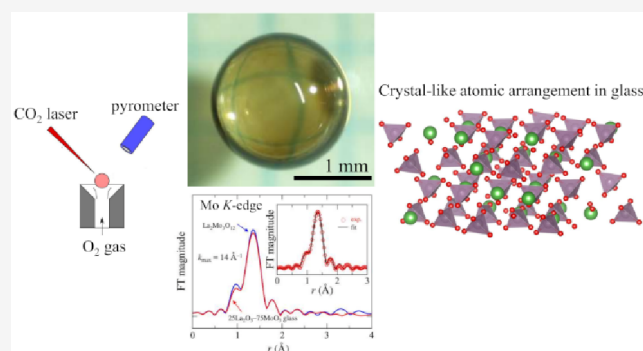
INTRODUCTION

Oxide glasses are constructed on a three-dimensional network of MO_n polyhedra where element M and oxygen (O) are bonded covalently. The constraints in glass formation are that the oxygen coordination number, n, should be as small as three or four, and that the MO_n polyhedra are connected to each other not by edge- or face-sharing but by corner-sharing. SiO$_2$, P$_2$O$_5$, etc., can form corner-sharing MO_4 tetrahedral networks, and they are thus referred to as network former oxides. Modifier oxides, such as alkali metal oxides, alkaline earth metal oxides, and rare earth oxides, typically break the network and introduce nonbridging oxygens. Al$_2$O$_3$, TiO$_2$, Nb$_2$O$_5$, and other intermediate oxides act as either a network former or modifier, depending on their composition in a glass.[1,2] In addition, among the intermediate oxides that cannot vitrify without additives, Al$_2$O$_3$, Ga$_2$O$_3$, MoO$_3$, and WO$_3$ can vitrify relatively easily, even at a binary composition, in combination with a specific modifier or intermediate. They are especially called conditional glass formers.[3] The glass-forming region of the binary system that includes conditional glass formers is generally narrow. Nevertheless, an additional small amount of network former oxide added to a binary system drastically improves the glass-forming ability.

MoO$_3$ is a conditional glass former, and glass formation in some of its binary systems has been reported. However, compared to Al$_2$O$_3$- and Ga$_2$O$_3$-based binary glasses, the number of reports is considerably small. Nassau et al. prepared Li$_2$O−MoO$_3$ binary glasses during a search for glasses with high ionic conductivity in the 1980s.[4] However, glass formation required the use of the twin-roller quenching method with a very high cooling rate (10^4−10^6 K/s). Ag$_2$O−MoO$_3$ binary glasses with a thickness of approximately 1 mm were obtained by a conventional melt-quench method to investigate their ionic conductivity.[5] Recent structural analysis combined with X-ray and neutron diffraction revealed that the coordination number of Mo decreased from 5.4 to 4.2 with increasing Ag$_2$O content and a variety of MoO$_n$ polyhedra (n = 4, 5, and 6) connected to each other to develop the network structure.[6] Dimitriev et al. have fabricated a variety of binary
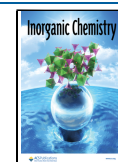
and ternary glasses that included MoO_3 as a main component since the 1990s and summarized a large amount of research on nontraditional molybdate glasses.[7−9] They succeeded in the glass formation of the $10La_2O_3−10Nd_2O_3−80MoO_3$ and $10R_2O_3−90MoO_3$ systems (R = La or Nd) using slow cooling rates (10^2 K/s). It was reported that the $10La_2O_3−90MoO_3$ glass had the glass transition temperature at around 325 °C and crystallization temperature at 410 °C. From structural analysis using Fourier transform infrared (FT-IR) and X-ray absorption fine structure (XAFS) spectroscopies, it was suggested that the glass network was build up with corner-sharing MoO_6 or MoO_5 without short isolated Mo=O bonds.[9]

A levitation technique is an effective method to vitrify a composition without a sufficient network former oxide in bulk form despite its low glass-forming ability. Various unconventional oxide glasses have been fabricated recently using a levitation technique in the last 20 years.[10−13] New glass compositions and the expansion of the glass-forming region were reported in systems with conditional glass formers as the main component. $R_2O_3−Al_2O_3$ glasses have very high elastic moduli,[14,15] and $R_2O_3−Ga_2O_3$ and $R_2O_3−WO_3$ glasses exhibit good optical properties such as infrared transparency, strong luminescence, and high refractive index with low wavelength dispersion.[16−19] In this study, $La_2O_3−MoO_3$ binary glasses were successfully obtained by a levitation technique in the bulk form. Physical properties of the binary glasses, including thermal and optical properties, were measured. Structural analysis using Mo L_3-edge, K-edge, and La L_3-edge XAFS and Raman scattering spectroscopies were performed to investigate the atomic arrangement of the glass by comparing it with the crystalline phase structure with the same composition as the glass.

■ EXPERIMENTAL PROCEDURE

Glass syntheses of the $(100−x)La_2O_3−xMoO_3$ binary system were examined by a levitation technique. High purity La_2O_3 and MoO_3 were stoichiometrically mixed and pressed into pellets. The pellets were sintered at 600 °C for 12 h in air and then were crushed to target pieces for the aerodynamic levitation (ADL) furnace. A piece of the target was placed on the nozzle of the ADL furnace and levitated by an O_2 gas flow. A CO_2 laser was used to melt the levitated sample for several seconds. The melt was rapidly cooled to room temperature by turning off the laser power, and then it solidified. The cooling rate was estimated to be approximately 500 °C/sec. Glass formation was confirmed by Cu $K\alpha$ X-ray diffraction measurements (XRD: Rigaku, MiniFlex600). Although the size of the fabricated glasses was approximately 2 mm, the thermal, optical, and structural properties could be sufficiently investigated. Crystalline $La_2Mo_3O_{12}$ as a reference was prepared by conventional solid-state reaction. High purity La_2O_3 and MoO_3 were stoichiometrically mixed and pressed into a pellet, and it was sintered in air at 800 °C for 24 h several times with intermediate pulverization.

The glass transition temperature (T_g) and crystallization temperature (T_x) for the glasses were investigated by using differential scanning calorimetry (DSC: NETZSCH, DSC 404 F1 Pegasus). The temperature was raised from room temperature to 700 °C with a heating rate of 10 °C/min in a N_2 gas flow. Prior to measurement of the physical properties, the glasses were annealed at 475 °C for 5 min to remove any internal stresses. Furthermore, post annealing of the glass in an oxidized atmosphere was conducted to diminish Mo^{5+} and improve transparency at the 400−600 nm region. The glasses were annealed in an O_2 gas flow at 400 °C for 24 h. The density of the glasses was measured using a He-gas pycnometer (micromeritics, AccupycII 1340). More than a dozen glass beads were placed in a 0.1 cc sample cell to reduce experimental errors.

Mo L-edge XAFS measurements were performed at the soft X-ray beamline, BL-10, in the SR Center of Ritsumeikan University.[20] The incident X-ray was monochromated with a double crystal using Ge(111) planes. Powdered samples of glasses and reference crystals were put on the carbon seal on the sample holder in a high vacuum chamber. The X-ray absorption spectra were recorded with the fluorescence yield method. Photon energy was calibrated at the energy of a peak (2481.69 eV) of white line of S K-edge XANES spectra of K_2SO_4 standard samples.

Mo K-edge and La L_3-edge XAFS spectra were recorded in transmission mode using two ionization chambers at the BL27B and BL9A beamlines in KEK-PF, respectively.[21−23] The incident X-ray was monochromated with a double crystal by using Si(111) planes. The samples were ground into powders and mixed with a high purity hexagonal boron nitride powder to form pellet specimens. Energy calibration for Mo K-edge spectra was performed by setting the inflection point of the spectra of a metallic Mo foil as E = 20003.9 eV and that for the La L_3-edge was done by setting the energy of the pre-edge peak of the Ti K-edge of a metallic Ti foil as E = 4966.0 eV. XAFS data analysis was conducted using the Athena and Artemis programs in the Demeter software package.[24] The k^3-weighting EXAFS spectra were Fourier-transformed (FT) to real space. Structural parameters regarding the first peak in the FT magnitude, such as the oxygen coordination number of Mo and La, the cation−oxygen distance, and the Debye−Waller (DW) factor, including both structural and thermal disorder, were evaluated by curve fitting analysis using phases and amplitude functions calculated using the FEFF8 code.

Unpolarized Raman scattering spectra of the glasses and crystalline $La_2Mo_3O_{12}$ were obtained in a 180°-scattering geometry by a confocal Raman microscope (JASCO, NRS-4500). The incident source was a 532 nm semiconductor laser.

For transmittance measurements, both sides of the glass samples were optically polished to a thickness of approximately 500 μm. Transmittance spectra were obtained using an ultraviolet−visible (UV−vis) spectrometer (Shimadzu, UV3600 plus) in the range of 250−2000 nm and an FTIR spectrometer (Shimadzu, IRAffinity-1S) in the range of 2000−10000 nm. The diffuse reflectance spectra of powder samples were also obtained using an integrating sphere installed in a UV3600 plus. $BaSO_4$ was used as a reference.

■ RESULTS AND DISCUSSION

The glass synthesis results are shown on the $La_2O_3−MoO_3$ binary phase diagram[25] in Figure 1. Bulk glasses were obtained only at x = 75 and 80 in the composition of the $(100−x)La_2O_3−xMoO_3$. Note that the x = 75 glass has the same composition as that of crystalline $La_2Mo_3O_{12}$. The glasses were homogeneously transparent and brownish colored, as shown in

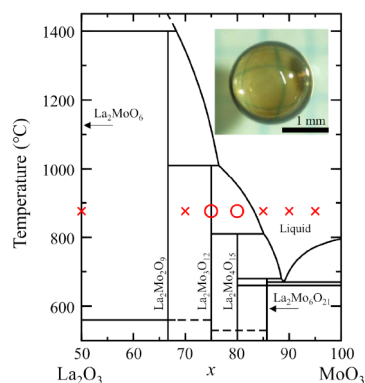**Figure 1.** Glass-forming range indicated on the $(100−x)La_2O_3−xMoO_3$ phase diagram. Circles and crosses indicate glass formation and crystallization, respectively. The inset shows a picture of the $25La_2O_3−MoO_3$ glass annealed in an O_2 gas flow at 400 °C in 24 h.

the inset. The glass-forming region of the $La_2O_3-MoO_3$ binary system is similar to that of the $La_2O_3-WO_3$ binary system.[19] The brown color of the $La_2O_3-MoO_3$ glasses is a unique characteristic compared to that of colorless $La_2O_3-WO_3$ glasses. The diameter of the spheric glasses was approximately 2 mm. At x = 50, 70, 85, 90, and 95, violent evaporation occurred during melting, and the targets were not vitrified. The glass formation in this study is clearly different from the previous report that showed glass formation with x = 90 using the conventional melt-quench method.[7,8,9] Glass formation at x = 90 rarely succeeded in our levitation experiments, but only where the melting time was long and the melting temperature was high. This may be due to composition deviation, resulting in an increase of La_2O_3 content because of MoO_3 volatilization.

Figure 2 shows the DSC curve of the x = 75 glass. The crystallization temperature, T_X, was found at 546 °C, and the
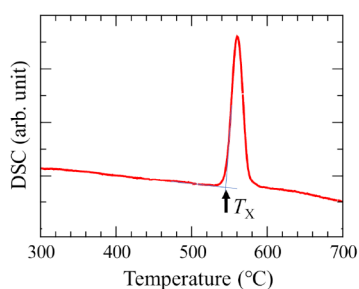

Figure 2. DSC curve of $25La_2O_3-75MoO_3$ glass.

crystallization peak was remarkably sharp. T_X of the x = 75 glass was lower than those of $20La_2O_3-80WO_3$ glass, which was at 594 °C. Determining the glass transition temperature was challenging due to minimal change in heat flow. Previous reports based on differential thermal analysis (DTA) data of the x = 90 glass indicated a crystallization peak temperature at 410 °C, and a subtle change, assumed to be T_g, was observed at approximately 325 °C.[7,9] However, no significant signal was observed in the temperature range from 300 °C to T_X in this study. Two possible reasons explain why the glass transition temperature was not detectable. One possibility is that T_g might be so close to T_X that T_g is obscured by the onset of the crystallization peak. Another possibility is that the difference in specific heat between the glassy state and supercooled liquid might be too small to be detected.

Figure 3 shows XRD profiles of the as-melted sample of x = 75, the crystallized sample after DSC measurement, and a calculated profile using the crystal structure of $La_2Mo_3O_{12}$.[26] The profile of the as-melted sample does not have any peaks, indicative of an amorphous nature. It is clearly shown that the profile of the crystallized sample is almost identical to the calculated profile of $La_2Mo_3O_{12}$. This implies that the atomic arrangement of x = 75 glass and crystalline $La_2Mo_3O_{12}$ may resemble each other. The crystal structure of $La_2Mo_3O_{12}$ is shown in the inset of Figure 3. There are five Mo sites and three La sites in the $La_2Mo_3O_{12}$ unit cell. The Mo atom forms highly isolated MoO_4, without any Mo−O−Mo connections, while the La atom is coordinated by eight oxygens. It can be seen that the MoO_4 tetrahedra connect at all four oxygen with LaO_8 by corner-sharing. Each of the six oxygens in LaO_8 is shared with MoO_4 at the corner, and each of the remaining two oxygens is shared by MoO_4 and two edge-shared LaO_8.
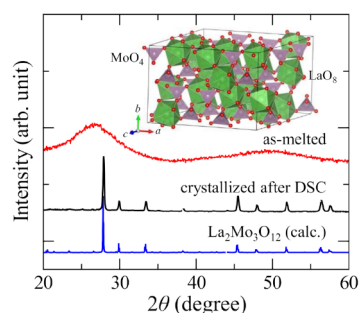

Figure 3. XRD profiles of the as-melted $25La_2O_3-75MoO_3$ sample and the crystallized sample after DSC measurement. The calculated profile of $La_2Mo_3O_{12}$ is shown at the bottom. The inset shows the crystal structure of $La_2Mo_3O_{12}$ drawn using VESTA software.[27] Purple and green polyhedra in the inset represent MoO_4 and LaO_8, respectively.

Alternatively, Mo^{6+} forms isolated MoO_4^{2-}, all of whose oxygen atoms are nonbridging, and La^{3+} coordinates it as a charge compensator.

The density of the x = 75 glass was measured to be 4.67 g/cm^3, indicating a 4.1% deviation from the calculated value of 4.87 g/cm^3 of $La_2Mo_3O_{12}$. The packing density (PD) was calculated using the equation PD = V_P/V_m, where V_P is the sum of the volume of component ions and V_m is the molar volume of the glass. Assuming that ions in the glass are spherical, the volume of the ith ion is expressed as $4\pi r_i^3/3$, where r_i represents the ionic radius of the ith ion. Shannon's ionic radii were utilized for volume calculations: 1.16 Å for La^{3+}(VIII), 0.41 Å for Mo^{6+}(IV), and 1.35 Å for O^{2-}(II).[28] The PD of the $25La_2O_3-75MoO_3$ glass was determined to be 0.510, closely resembling 0.532 of the $La_2Mo_3O_{12}$ crystal. Such similarity in PD between glass and crystalline phase, often observed in glasses prepared by a levitation technique,[29] suggests that the glass structure is highly packed, akin to the crystalline phase.

X-ray absorption near edge spectroscopy (XANES) spectra mainly originate from a superposition of electronic transitions and provide information on valence and chemical states of the elements to be measured. The relative height and position of the pre-edge peak in XANES spectra are often helpful to estimate the coordination number and distortion of the polyhedron.[30−32] XANES analyses for Mo were reported for silicate glasses and melts by comparing a variety of reference crystals.[33] XANES spectral shape and the pre-edge peak of the reference crystals strongly depend on the atomic arrangements and the valence state of Mo. Linear correlation was clearly shown between the average valence state of Mo and the Mo K-edge position at a normalized absorbance equal to one. The XANES spectra of silicate glasses also showed this variation; however, the degree of difference is much smaller than the case of crystalline phases. It was concluded that the valence state of Mo was six in silicate glasses prepared in ambient conditions, and the reduction of Mo requires a strong reduced condition. The coordination number of Mo estimated from the pre-edge peaks is almost four; however, there are some glasses with higher coordination numbers, ranging from 4 to 6 even in silicate glasses.[33]

Mo K-edge XAFS spectra of the $La_2O_3-MoO_3$ binary system were clearly different from silicate glasses, and they provide clear evidence of the similarity of local structure around Mo atoms between glassy and crystalline phases. Figure

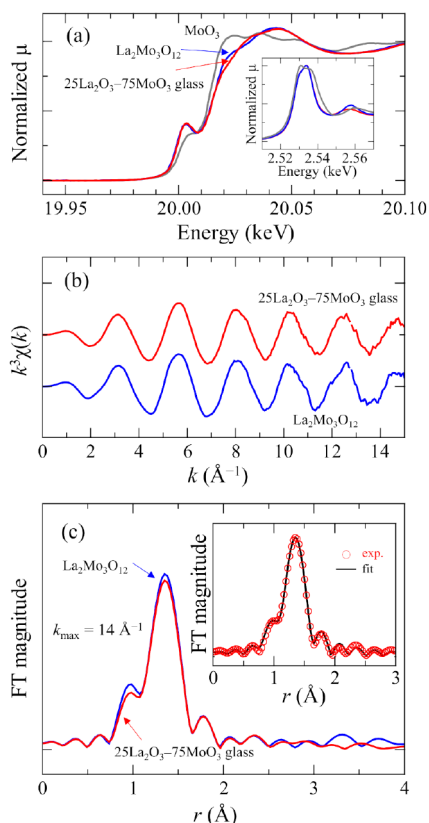4a shows Mo K-edge XANES spectra of the $25La_2O_3-75MoO_3$ glass and $La_2Mo_3O_{12}$ with reference MoO_3. Mo in

Figure 4. Mo K-edge XAFS spectra of $25La_2O_3-75MoO_3$ glass and crystalline $La_2Mo_3O_{12}$. (a) XANES spectra, (b) k^3-weighted EXAFS spectra, and (c) the FT magnitude of EXAFS oscillation. Inset of (a) shows Mo L_3-edge XANES spectra. Inset of (c) shows the fitting result of the glass.

MoO_3 has a valence state of 6+ and is coordinated by six oxygen atoms. MoO_6 polyhedra are connected to each other by sharing corners and edges. The spectrum of the glass is clearly different from that of MoO_3, especially at the pre-edge region; however, it is almost the same as that of $La_2Mo_3O_{12}$. Compared to MoO_3, the pre-edge peak of the glass is higher, and the position shifted to the lower energy side, indicating that Mo forms MoO_4 tetrahedra as well as $La_2Mo_3O_{12}$. From the absorption edge energy, Mo in the glass is estimated to be 6+, as well as that in the two reference crystals.

Mo L_3-edge XANES spectrum, in which the peaks are mainly ascribed to the transition from $2p$ to $4d$ states, is helpful to predict the oxygen coordination number of Mo as well as K-edge XANES spectrum.[34] Mo L_3-edge XANES spectra of the glass and reference crystals are shown in the inset of Figure 4a. Two peaks were clearly observed in the spectra of MoO_3. The peak at the higher energy side was less intense than that on the lower energy side, implying that they are associated with the e_g and t_{2g} empty states of octahedral MoO_6. The spectra of the glass and crystalline $La_2Mo_3O_{12}$ were almost the same shape, which is evidence of the local structural similarity between them. The main peak consists of two peaks with an energy difference smaller than that of the MoO_3 spectrum. The intensity ratio of the peak at the higher energy side and lower side was the opposite of that of MoO_3. These results suggest

that the two peaks are attributed to the electron transition in the tetrahedral crystal field splitting.

Figure 4b shows the k^3-weighted EXAFS spectra, $k^3\chi(k)$ of the $25La_2O_3-75MoO_3$ glass and crystalline $La_2Mo_3O_{12}$. The oscillation was observed clearly in a high k range. The glass and crystal are almost the same in shape and intensity. This means the homogeneity and uniformity of the local structure around Mo in the glass. Figure 4c shows the FT amplitude of the k^3-weighted EXAFS spectra with $k_{max} = 14.0$ Å^{-1}. They are almost the same; however, a relatively smaller peak height was observed for the glass, indicating a slightly smaller coordination number or disorder in atomic arrangement around Mo. Furthermore, there is no correlation at 3.8−4.0 Å for the second nearest shell in the glass, while a small but clear correlation is observed in the crystal, showing disorder in the glass. A correlation smaller than expected from the FEFF calculation is often observed in molybdate crystalline phases, such as Na_2MoO_4 and Ag_2MoO_4.[33,35]

In order to more quantitatively investigate the local structure around the Mo, fitting of the K-edge EXAFS spectra was performed. Prior to the fitting of EXAFS spectra for the glass, it is necessary to determine the inelastic multielectronic losses, S_0^2, of the EXAFS formula in this experiment from the fitting result of a reference crystal. The fitting for $La_2Mo_3O_{12}$ was performed in the r range from 1 to 2 Å with a fixed value of 4.0 for the coordination number, N. The value of S_0^2 was 0.885. The Mo−O distance, R, and DW factor, σ^2, are 1.778 ± 0.002 and 0.0022 ± 0.0002 Å^2, respectively, as shown in Table 1. The

Table 1. Parameters Used to Fit the Mo K-edge EXAFS Spectra of $25La_2O_3-75MoO_3$ Glass and Crystalline $La_2Mo_3O_{12}$

	N	R (Å)	σ^2	ΔE (eV)
$25La_2O_3-MoO_3$ glass	3.9(1)	1.778(2)	0.0022(2)	2.1(7)
crystalline $La_2Mo_3O_{12}$	4.0[a]	1.778(2)	0.0022(2)	2.4(7)

[a]Fixed value, $S_0^2 = 0.885$.

fitting of the glass was performed by using the S_0^2 value. The coordination numbers of Mo, R, and σ^2 were 3.9 ± 0.1, 1.778 ± 0.002 Å, and 0.0022 ± 0.0002 Å^2, which are almost the same as that of $La_2Mo_3O_{12}$. The coordination number of the glass certainly smaller than that of the crystal but they are almost the same within an error. It should be noted that there is almost no difference in the structural parameters N, R, and σ^2 between the glass and crystal, which strongly indicates the similarity in the local structure of the Mo atom in the first coordination shell. Therefore, it is highly estimated that Mo in the glass forms regular tetrahedra with four nonbridging oxygens as in the case of $La_2Mo_3O_{12}$.

Figure 5 shows La L_3-edge XAFS spectra of $25La_2O_3-75MoO_3$ glass and crystalline $La_2Mo_3O_{12}$. In contrast to Mo K-edge XAFS, there is a clear difference between the glass and the crystal. The peak height of the white line in the glass XANES spectrum is clearly smaller than that of the crystal, and the oscillation above 5.50 eV for the glass is not obvious compared to the crystal (Figure 5a). This is indicative of the disordered structure of the glass. Figure 5b shows EXAFS spectra of the glass and the crystal. The intensity of the glass is much smaller than the crystal; however, the oscillation periods are similar to each other, indicative of local environment similarity around the La atoms. Because the La L_2-edge absorption is nearly located, there is a limited k range available
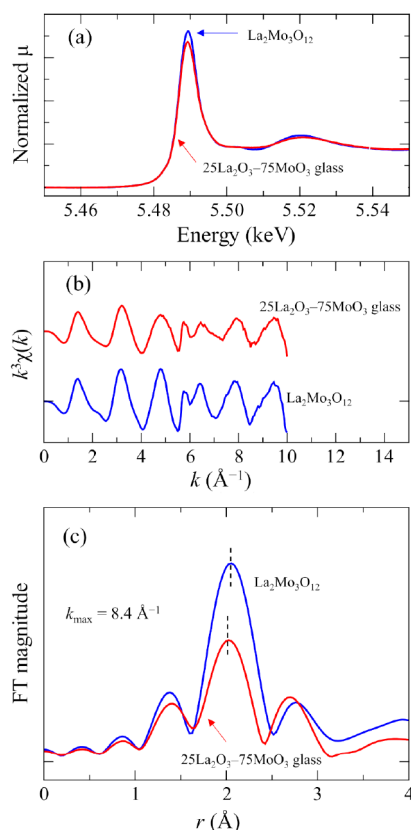
Figure 5. La L_3-edge XAFS spectra of $25La_2O_3-75MoO_3$ glass and crystalline $La_2Mo_3O_{12}$. (a) XANES spectra, (b) k^3-weighted EXAFS spectra, and (c) the FT magnitude of the EXAFS oscillation.

for FT of the EXAFS spectra. Figure 5c shows the FT magnitudes of the glass and the crystal. Because of the limited range of k (3 Å^{-1} ≤ k ≤ 8.4 Å^{-1}), it is difficult to estimate structural parameters by fitting. From the simple fitting of crystalline spectra with a fixed coordination number value of eight, the inelastic multielectronic loss, S_0^2, is estimated to be 0.95, and the La−O distance R and DW factor σ^2 are 2.48 ± 0.02 Å and 0.007 ± 0.001 Å^2, respectively. By using the S_0^2 value, the coordination number of La, R, and σ^2 for the glass were 6.4 ± 0.1, 2.46 ± 0.01 Å, and 0.009 ± 0.002 Å^2, respectively. The La−O bond length of the glass is slightly shorter than that of the crystal. The apparent small coordination number of glass might be due to disorder in the atomic arrangement and does not indicate that the number of oxygen atoms around La in the glass is smaller than that of the crystal. The disorder sometimes diminishes the longer side peak by averaging the distribution in amorphous materials. Accordingly, XAFS analysis using Mo K-edge and La L_3-edge absorptions indicates structural similarity around Mo and La between the glass and crystal, although disorder is obvious, especially around La in the glass.

Further evidence of the structural similarity between the glass and the crystal is clearly shown in the vibration spectra. Figure 6 shows Raman scattering spectra of the glass and the crystal. It should be noted that the spectrum of glass clearly resembles the crystalline spectrum in peak position and peak height. It seems that broadening the spectrum of the crystal matches well with that of the glass. The agreement of the glass and the crystal strongly suggests that the local environment around the Mo atoms, such as the bonding distance to oxygen,
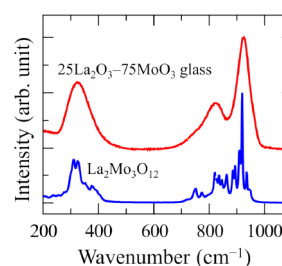

Figure 6. Raman scattering spectra of $25La_2O_3-75MoO_3$ glass and crystalline $La_2Mo_3O_{12}$.

the oxygen coordination number, and the oxygen−cation−oxygen bond angles, is almost the same. Detailed analyses of Raman bands of crystals including Mo have been reported in the literature.[36−38] The bands at 880−970 cm^{-1} and 750−880 cm^{-1} are attributed to the Mo−O symmetric stretching mode and antisymmetric stretching modes in MoO_4 tetrahedra, respectively. The band at 320 cm^{-1} is attributed to the O−Mo−O bending mode in MoO_4 tetrahedra.

Finally, the optical properties of the glass are shown in Figure 7. Figure 7a shows the transmittance spectra of the x =
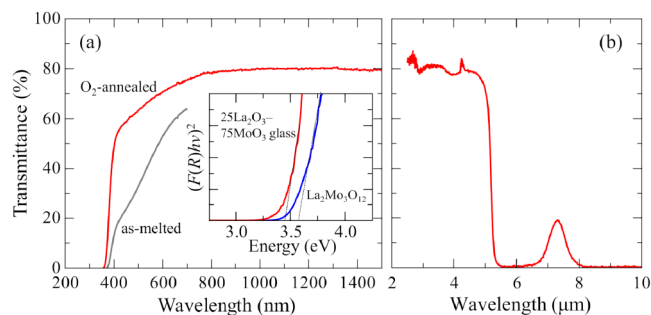

Figure 7. (A) UV−vis transmittance spectra of $25La_2O_3-75MoO_3$ glasses. Red line represents the glass annealed in O_2 gas flow, while gray line represents the as-melted glass. (Inset) Tauc plot using the Kubelka−Munk function, $F(R)$, obtained from diffuse scattering spectra of $25La_2O_3-75MoO_3$ glass and crystalline $La_2Mo_3O_{12}$. The factor m is 1/2. (b) IR transmittance spectra of a $25La_2O_3-75MoO_3$ glass.

75 glasses in the UV−vis region. Compared with the spectrum of the as-melted glass, the transparency of the glass annealed in the O_2 gas flow was improved in the visible range. The UV absorption edge is approximately 378 nm, from which the optical bandgap energy is estimated to be 3.40 eV. The small absorption at 400−700 nm is obvious, which might be due to the d−d transition in Mo^{5+}. The amount of Mo^{5+} should be very small because it was difficult to find evidence of a lower valence state of Mo in the Mo K-edge XANES spectra. The maximum transmittance was 80% at 1000 nm, which can be attributed to reflection on both sides of the surface during the measurement. Assuming that there is only surface reflection and no light scattering inside the glass, the refractive index, n, of the glass is estimated to be 2.0 using the equation $T_{max} = 1 − [2R'/(1 + R')]$, where T_{max} is the maximum transmittance and $R' = [(n − 1)/(n + 1)]^2$. The estimated refractive index at 1000 nm is slightly larger than that of $20La_2O_3-80WO_3$ glass.[19] Since the optical bandgap energy of the x = 75 glass is not so large, the wavelength dispersion of the refractive index will be large, which is not suitable for lenses in the visible region. Nevertheless, the $La_2O_3-MoO_3$ glasses are possible

candidates for optical applications using high refractive index in the near-infrared region.

The optical absorption edge of the glass can be compared to that of the powdered crystalline phase using diffuse reflectance spectroscopy. The Kubelka−Munk function, $F(R)$, is obtained from the reflectance spectra. The Tauc method equation is transformed to eq 1 by substituting $F(R)$ for the absorption coefficient, α:

$$(F(R)h\nu)^{1/m} = B(h\nu - E_g) \tag{1}$$

where h is the Planck constant, ν is the photon frequency, E_g is the optical band gap energy, and B is a constant. The factor m depends on the nature of the electron transition and is equal to 1/2 or 2 for direct or indirect transition band gaps, respectively. The inset of Figure 7a shows the Tauc plot with $m = 1/2$ by using the Kubelka−Munk function. The Tauc plot curve of the glass clearly shifts to the lower energy side compared to that of the crystalline sample. The x-axis intersection point of the linear fit of the Tauc plot gives an optical band gap energy. The estimated E_g of the glass is 3.46 eV, which is in good agreement with the value obtained from transmittance spectra. The E_g of the crystalline sample is 3.60 eV.[39] The bandgap of the glass is slightly smaller than that of the crystal, which is reasonable considering the disorder in atomic arrangements characteristic to amorphous materials.

Figure 7b shows the infrared transmittance spectra of the glass. The glass was transparent to 5.5 μm, and the absorption at 2.9 μm is attributed to the presence of the O−H vibration. Compared with conventional oxide glasses, the O−H absorption of the glass is considerably small, indicating a scarcity of OH groups. Furthermore, there is the additional transmittance window in the range 6.5−8.0 μm. A transparent region at the wavelength side longer than the infrared absorption edge was also found in R-rich R_2O_3−B_2O_3 binary glasses (R is a rare earth element or Y).[40−42] The additional transmittance in the R-rich borate glasses was explained by considering the local structure around the B atoms. B atoms in the glass form isolated BO_3 units without any three-dimensional network structure. The simple environment around the B atoms resulted in the suppression of the overlap of the absorption bands of the B−O multiple vibrations and their overtones observed in conventional borate glasses. As a result, the absorption bands discretize, and then an additional transmittance window emerges. The local structure around the Mo atom in the $25La_2O_3$−$75MoO_3$ glass is confirmed to be the isolated MoO_4^{2-} from XAFS and Raman scattering spectra, which is seen in crystalline $La_2Mo_3O_{12}$. Therefore, the additional transmittance window at 6.5−8.0 μm can be explained by suppression of the overlap of the absorption bands of Mo−O multiple vibrations and their overtones because of the simple environment around Mo as in the case of crystalline $La_2Mo_3O_{12}$.

Crystallization of the glass, XAFS and Raman scattering spectra, and the additional infrared transmittance as mentioned above strongly indicate that the atomic arrangement of the $25La_2O_3$−$75MoO_3$ glass is almost the same as that of the crystalline $La_2Mo_3O_{12}$, even though structural disorder in the glass was confirmed in the La L_3-edge XAFS and the absorption edge in the UV−vis region. MoO_3 is classified as a conditional network former, and it has been reported that MoO_n ($n = 4$, 5, or 6) formed a network in MoO_3-based glasses.[5,6] Contrary to previously reported glasses, there is no

network in the La_2O_3−MoO_3 glasses and Mo forms completely isolated MoO_4^{2-}. Furthermore, the La_2O_3−MoO_3 glasses are highly packed and comparable to those of the crystalline phase. The highly dense packed structure and the structural similarity of the crystal are unique and distictive in glass science; however, similar results have been reported recently in glasses prepared by a levitation technique.[12,40] As suggested in the previous study, the structural similarity of the glass and the crystalline phases might enhance the glass-forming ability of the densely packed glass system. Assuming that R^{3+} and O^{2-} are arranged in the nearly closest packed structure and small cations, such as Mo^{6+} ions, are inserted into interstitial sites (tetrahedral sites in the case of La_2O_3−MoO_3 binary system) in the glass, the amorphous nature is produced by the slight displacement from the atomic arrangement of the crystalline phase. The small displacement enables a fall in metabasins in the free energy landscape[43,44] and thus loses long-range order in the case of densely packed glass systems.[45] In this case, glass formation becomes possible even when the three-dimensional regular tetrahedral networks are not developed.

■ SUMMARY

Bulk glass formation of the La_2O_3−MoO_3 binary system was achieved using the levitation technique. The glass-forming region was narrow at the vicinity of 25-mol % La_2O_3. The fabricated glasses were brownish but transparent in the visible region. The physical and structural properties of the $25La_2O_3$−$75MoO_3$ glass were investigated because competing crystalline phase of $La_2Mo_3O_{12}$ exists at the same composition. The glass transition temperature was not detected due to minimal change in heat flow, while the crystallization temperature was 546 °C. After the sharp crystallization peak, a single phase of $La_2Mo_3O_{12}$ crystallized. Mo L_3-edge and K-edge XAFS and Raman scattering spectra revealed structural similarity between the glass and the crystal. The glass is formed by isolated MoO_4^{2-} tetrahedra without any network formation. La L_3-edge XAFS and optical bandgap in the UV−vis range indicate the disorder in the atomic arrangement of the glass. An additional infrared transparent window at 6.5−8.0 μm was explained by the simple environment of the local structure around Mo, which has been commonly observed in highly packed glasses prepared by the levitation technique. The estimated refractive index of 2.0 at 1.0 um and broad infrared transparency open up the possibility of optical applications in the infrared range. Furthermore, it was suggested that the glass formation of the La_2O_3−MoO_3 system was caused by slight movement from the ordered $La_2Mo_3O_{12}$ structure and, thus, it does not require a three-dimensional tetrahedral network.

■ AUTHOR INFORMATION

Corresponding Author

Atsunobu Masuno − *Graduate School of Engineering, Kyoto University, Kyoto 615-8520, Japan; Graduate School of Science and Technology, Hirosaki University, Hirosaki, Aomori 036-8505, Japan; Institute of Industrial Science, The University of Tokyo, Tokyo 153-8505, Japan;* ⊙ orcid.org/0000-0003-0667-9782; Email: masuno.atsunobu.3k@kyoto-u.ac.jp

Authors

Sae Munakata − *Graduate School of Science and Technology, Hirosaki University, Hirosaki, Aomori 036-8505, Japan*

Inorganic Chemistry

pubs.acs.org/IC

Article

Yoshihiro Okamoto − *Materials Sciences Research Center, Japan Atomic Energy Agency, Sayo-gun, Hyogo 679-5148, Japan*

Toyonari Yaji − *Research Organization of Science and Technology, Ritsumeikan University, Kusatsu, Shiga 525-8577, Japan*

Yoshihisa Kosugi − *Institute for Chemical Research, Kyoto University, Uji, Kyoto 611-0011, Japan*

Yuichi Shimakawa − *Institute for Chemical Research, Kyoto University, Uji, Kyoto 611-0011, Japan;* ● orcid.org/0000-0003-1019-2512

Complete contact information is available at:
https://pubs.acs.org/10.1021/acs.inorgchem.4c00176

Notes

The authors declare no competing financial interest.

■ REFERENCES

(1) Zachariasen, W. H. The Atomic Arrangement in Glass. *J. Am. Chem. Soc.* **1932**, *54* (10), 3841−3851.

(2) Sun, K.-H. Fundamental Condition of Glass Formation. *J. Am. Ceram. Soc.* **1947**, *30* (9), 277−281.

(3) Rawson, H. *Inorganic Glass-Forming Systems*; Academic Press, 1967.

(4) Nassau, K.; Glass, A. M.; Grasso, M.; Olson, D. H. Rapidly Quenched Tungstate and Molybdate Composition Containing Lithium: Glass Formation and Ionic Conductivity. *J. Electrochem. Soc.* **1980**, *127* (12), 2743−2747.

(5) Bhattacharya, S.; Ghosh, A. Electrical Properties of Ion Conducting Molybdate Glasses. *J. Appl. Phys.* **2006**, *100* (11), 114119.

(6) Hoppe, U.; Schöps, A.; Hannon, A. C.; Ghosh, A. Structure of Silver Molybdate Glasses by X-Ray and Neutron Diffraction. *J. Non-Cryst. Solids* **2021**, *573*, 121143.

(7) Dimitriev, Y.; Iordanova, R. Non-Traditional Molybdate Glasses. *Phys. Chem. Glasses* **2009**, *50* (2), 123−132.

(8) Dimitriev, Y.; Iordanova, R.; Aleksandrov, L.; Kostov, K. L. Boromolybdate Glasses Containing Rare Earth Oxides. *Phys. Chem. Glasses* **2008**, *50* (3), 212−218.

(9) Aleksandrov, L.; Iordanova, R.; Dimitriev, Y. B.; Handa, K.; Ide, J.; Milanova, M. Glass Formation in the MoO₃-La₂O₃-Nd₂O₃ System. *Adv. Mater. Res.* **2008**, *39−40*, 37−40.

(10) Weber, J. K. R. The Containerless Synthesis of Glass. *Int. J. Appl. Glass Sci.* **2010**, *1* (3), 248−256.

(11) Benmore, C. J.; Weber, J. K. R. Aerodynamic Levitation Supercooled Liquids and Glass Formation. *Adv. Phys.: X* **2017**, *2* (3), 717−736.

(12) Masuno, A. Structure of Densely Packed Oxide Glasses Prepared Using a Levitation Technique. *J. Phys. Soc. Jpn.* **2022**, *91* (9), 091003.

(13) Masuno, A. Functionalities in Unconventional Oxide Glasses Prepared Using a Levitation Technique. *J. Ceram. Soc. Jpn.* **2022**, *130* (8), 563−574.

(14) Watanabe, Y.; Masuno, A.; Inoue, H. Glass Formation of Rare Earth Aluminates by Containerless Processing. *J. Non-Cryst. Solids* **2012**, *358* (24), 3563−3566.

(15) Rosales-Sosa, G. A.; Masuno, A.; Higo, Y.; Watanabe, Y.; Inoue, H. Effect of Rare-earth Ion Size on Elasticity and Crack Initiation in Rare-earth Aluminate Glasses. *J. Am. Ceram. Soc.* **2018**, *101* (11), 5030−5036.

(16) Yoshimoto, K.; Masuno, A.; Ueda, M.; Inoue, H.; Yamamoto, H.; Kawashima, T. Low Phonon Energies and Wideband Optical Windows of La₂O₃-Ga₂O₃ Glasses Prepared Using an Aerodynamic Levitation Technique. *Sci. Rep.* **2017**, *7* (1), 45600.

(17) Yoshimoto, K.; Ezura, Y.; Ueda, M.; Masuno, A.; Inoue, H. 2.7 Mm Mid-Infrared Emission in Highly Erbium-Doped Lanthanum Gallate Glasses Prepared Via an Aerodynamic Levitation Technique. *Adv. Opt. Mater.* **2018**, *6* (8), 1701283.

(18) Yoshimoto, K.; Ezura, Y.; Ueda, M.; Masuno, A.; Inoue, H.; Mizuguchi, M. Fluorescence Characterization of Heavily Eu³⁺-Doped Lanthanum Gallate Glass Spheres with High Quenching Concentration. *Opt. Lett.* **2019**, *44* (4), 875−878.

(19) Yoshimoto, K.; Masuno, A.; Inoue, H.; Watanabe, Y. Transparent and High Refractive Index La₂O₃−WO₃ Glass Prepared Using Containerless Processing. *J. Am. Ceram. Soc.* **2012**, *95* (11), 3501−3504.

(20) Nakanishi, K.; Yagi, S.; Ohta, T. XAFS Measurements under Atmospheric Pressure in the Soft X-ray Region. *AIP Conf. Proc.* **2010**, *1234*, 931.

(21) Nomura, M.; Koyama, A. Design of an XAFS Beamline at the Photon Factory: Possibilities of Bent Conical Mirrors. *J. Synchrotron Rad.* **1999**, *6* (PT 3), 182−184.

(22) Nomura, M.; Koyama, A. Performance of a Beamline with a Pair of Bent Conical Mirrors. *Nucl. Instr. Methods Phys. Res. A* **2001**, *467−468*, 733−736.

(23) Konishi, H.; Yokoya, A.; Shiwaku, H.; Motohashi, H.; Makita, T.; Kashihara, Y.; Hashimoto, S.; Harami, T.; Sasaki, T. A.; Maeta, H.; Ohno, H.; Maezawa, H.; Asaoka, S.; Kanaya, N.; Ito, K.; Usami, N; Kobayashi, K. Synchrotron Radiation Beamline to Study Radioactive Materials at the Photon Factory. *Nucl. Instr. Methods Phys. Res. A* **1996**, *372* (1−2), 322−332.

(24) Ravel, B.; Newville, M. *ATHENA, ARTEMIS, HEPHAESTUS*: Data Analysis for X-Ray Absorption Spectroscopy Using *IFEFFIT*. *J. Synchrotron Rad.* **2005**, *12* (4), 537−541.

(25) Rode, E. Y.; Lysanova, G. V.; Gokhman, L. Z. Phase Diagrams of the Systems of Rare Earths Oxides with Molybdenum Trioxide. *Izv. Akad. Nauk SSSR, Neorg. Mater.* **1971**, *7*, 2101−2103.

(26) Jeitschko, W. Crystal Structure of La₂(MoO₄)₃, a New Ordered Defect Scheelite Type. *Acta Crystallogr., Sect. B: Struct. Crystallogr. Cryst. Chem.* **1973**, *29* (10), 2074−2081.

(27) Momma, K.; Izumi, F. VESTA 3 for Three-Dimensional Visualization of Crystal, Volumetric and Morphology Data. *J. Appl. Crystallogr.* **2011**, *44* (6), 1272−1276.

(28) Shannon, R. D. Revised Effective Ionic Radii and Systematic Studies of Interatomic Distances in Halides and Chalcogenides. *Acta Crystallogr. A* **1976**, *32* (5), 751−767.

(29) Masuno, A.; Inoue, H.; Yoshimoto, K.; Watanabe, Y. Thermal and Optical Properties of La₂O₃-Nb₂O₅ High Refractive Index Glasses. *Opt. Mater. Express* **2014**, *4* (4), 710−718.

(30) Farges, F.; Brown, G. E.; Petit, P.-E.; Munoz, M. Transition Elements in Water-Bearing Silicate Glasses/Melts. Part I. a High-Resolution and Anharmonic Analysis of Ni Coordination Environments in Crystals, Glasses, and Melts. *Geochim. Cosmochim. Acta* **2001**, *65* (10), 1665−1678.

(31) Farges, F. *Ab Initio* and Experimental Pre-Edge Investigations of the Mn K -Edge XANES in Oxide-Type Materials. *Phys. Rev. B* **2005**, *71* (15), 155109.

(32) Chalmin, E.; Farges, F.; Brown, G. E. A Pre-Edge Analysis of Mn K-Edge XANES Spectra to Help Determine the Speciation of Manganese in Minerals and Glasses. *Contrib. Mineral. Petrol.* **2009**, *157* (1), 111−126.

(33) Farges, F.; Siewert, R.; Brown, G. E., Jr.; Guesdon, A.; Morin, G. Structural Environments Around Molybdenum in Silicate Glasses and Melts. I. Influence of Composition and Oxygen Fugacity on the Local Structure of Molybdenum. *Can. Mineral.* **2006**, *44* (3), 731−753.

(34) Aritani, H.; Tanaka, T.; Funabiki, T.; Yoshida, S.; Eda, K.; Sotani, N.; Kudo, M.; Hasegawa, S. Study of the Local Structure of Molybdenum−Magnesium Binary Oxides by Means of Mo L$_3$-Edge XANES and UV−Vis Spectroscopy. *J. Phys. Chem.* **1996**, *100* (50), 19495−19501.

(35) Rocca, F.; Kuzmin, A.; Mustarelli, P.; Tomasi, C.; Magistris, A. XANES and EXAFS at Mo K-Edge in (AgI)$_{1−x}$(Ag$_2$MoO$_4$)$_x$ Glasses and Crystals. *Solid State Ionics* **1999**, *121* (1−4), 189−192.

(36) Ait Ahsaine, H.; Zbair, M.; Ezahri, M.; Benlhachemi, A.; Bakiz, B.; Guinneton, F.; Gavarri, J.-R. Structural and Temperature-Dependent Vibrational Analyses of the Non-Centrosymmetric ZnMoO$_4$ Molybdate. *J. Mater. Environ. Sci.* **2016**, *7* (9), 3076−3083.

(37) McKeown, D. A.; Gan, H.; Pegg, I. L. X-Ray Absorption and Raman Spectroscopy Studies of Molybdenum Environments in Borosilicate Waste Glasses. *J. Nucl. Mater.* **2017**, *488*, 143−149.

(38) Stenzel, D.; Issac, I.; Wang, K.; Azmi, R.; Singh, R.; Jeong, J.; Najib, S.; Bhattacharya, S. S.; Hahn, H.; Brezesinski, T.; Schweidler, S.; Breitung, B. High Entropy and Low Symmetry: Triclinic High-Entropy Molybdates. *Inorg. Chem.* **2021**, *60* (1), 115−123.

(39) Wang, Q.; Liao, M.; Lin, Q.; Xiong, M.; Zhang, X.; Dong, H.; Lin, Z.; Wen, M.; Zhu, D.; Mu, Z.; Wu, F. The Design of Dual-Switch Fluorescence Intensity Ratio Thermometry with High Sensitivity and Thermochromism Based on a Combination Strategy of Intervalence Charge Transfer and up-Conversion Fluorescence Thermal Enhancement. *Dalton Trans.* **2021**, *50* (26), 9298−9309.

(40) Masuno, A.; Iwata, T.; Yanaba, Y.; Sasaki, S.; Inoue, H.; Watanabe, Y. High Refractive Index La-Rich Lanthanum Borate Glasses Composed of Isolated BO$_3$ Units. *Dalton Trans.* **2019**, *48* (29), 10804−10811.

(41) Sasaki, S.; Masuno, A.; Ohara, K.; Yanaba, Y.; Inoue, H.; Watanabe, Y.; Kohara, S. Structural Origin of Additional Infrared Transparency and Enhanced Glass-Forming Ability in Rare-Earth-Rich Borate Glasses without B−O Networks. *Inorg. Chem.* **2020**, *59* (19), 13942−13951.

(42) Sasaki, S.; Masuno, A. Composition dependence of the local structure and transparency of Gd$_2$O$_3$−B$_2$O$_3$ binary glasses prepared via aerodynamic levitation. *J. Ceram. Soc. Jpn.* **2022**, *130* (1), 60−64.

(43) Greaves, G. N.; Sen, S. Inorganic Glasses, Glass-Forming Liquids and Amorphizing Solids. *Adv. Phys.* **2007**, *56* (1), 1−166.

(44) Pérez-Castañeda, T.; Jiménez-Riobóo, R. J.; Ramos, M. A. Two-Level Systems and Boson Peak Remain Stable in 110-Million-Year-Old Amber Glass. *Phys. Rev. Lett.* **2014**, *112* (16), 165901.

(45) Eguchi, T.; Inoue, H.; Masuno, A.; Kita, K.; Utsuno, F. Oxygen Close-Packed Structure in Amorphous Indium Zinc Oxide Thin Films. *Inorg. Chem.* **2010**, *49* (18), 8298−8304.